Articles

Mutations in Transmembrane Domains 5 and 7 of the Human Excitatory Amino Acid Transporter 1 Affect the Substrate-Activated Anion Channel†

Shiwei Huang and Robert J. Vandenberg*

Discipline of Pharmacology, Bosch Institute, University of Sydney, Sydney, New South Wales 2006, Australia

Received April 5, 2007; Revised Manuscript Received June 26, 2007

ABSTRACT: L-Glutamate is the predominant excitatory neurotransmitter in the brain, and its extracellular concentration is tightly controlled by the excitatory amino acid transporters (EAATs). The transport of 1 glutamate molecule is coupled to the cotransport of 3 Na^+ and 1 H^+ and the countertransport of 1 K^+. In addition to substrate transport, the binding of glutamate and Na^+ activates an anion current which is thermodynamically uncoupled from the transport process. We have identified three amino acid residues in EAAT1 (D272 in TM5, K384 and R385 in TM7) that influence the amplitude of the anion channel current relative to the transport current. Transporters containing the mutations R268A, D272A, D272K, K384A, K384D, R385A, and R385D were expressed in *Xenopus laevis* oocytes and their transport and anion channel functions measured using the two-electrode voltage clamp techniques. The D272, K384, and R385 mutant transporters showed no change in transport properties but have increased levels of anion channel activity compared to wild-type transporters. These results identify additional residues of the EAAT1 transporter that may contribute to the gating mechanism of the anion channel of glutamate transporters and also provide hints as to how substrate binding leads to channel activation.

Glutamate is the major excitatory neurotransmitter in the brain, and its uptake by glutamate transporters is the primary way of regulating its concentration in the synaptic cleft to maintain a dynamic signaling process between neurons (*1*). Glutamate transporters are secondary active transporters in which glutamate transport is coupled to the cotransport of 3 Na^+ and 1 H^+ and the countertransport of 1 K^+ ion, which allows the transporter to maintain a 10^6-fold glutamate concentration gradient across the cell membrane (*2*). Glutamate transporters are unusual proteins because, in addition to their role as secondary active transporters, these proteins also function as anion channels. It has recently been demonstrated that in rat retina bipolar cells binding of glutamate to a presynaptic glutamate transporter activates the anion conductance causing hyperpolarization of the presynaptic membrane and inhibits further glutamate release (*3*). Glutamate and Na^+ ions are required for gating of the anion channel, but the direction of anion flux through the transporter is uncoupled from the transport process (*4*). In addition to the predominant physiological anion, Cl^-, the channel is permeable to other monovalent anions with a relative permeability sequence of SCN^- being more permeant than ClO_4^- > NO^- > I^- > Br^- > Cl^- > F^- (*5*). The aim of this study was to identify amino acid residues that play a role in anion channel function.

The anion channel function of glutamate transporters is mediated by a different conformational state of the transporter to that which transports glutamate (*6*−*8*), and we have previously identified a number of amino acid residues within the second transmembrane (TM)[1] domain of the human glutamate transporter, EAAT1, that influence anion permeation through the transporter (*9*). In addition, a residue in the intracellular loop between TM2 and TM3, D112, may play a role in gating of the anion channel (*9*). It is interesting to note that mutations in TM2 that affect anion permeation do not appear to affect glutamate transport, which raises the question as to how does glutamate and Na^+ binding to the transporter lead to opening of the channel.

In 2004, a crystal structure of a bacterial aspartate transporter, Glt_{Ph}, was published (*10*), and subsequently the structure of a blocker-bound conformation was determined (*11*). The amino acid sequence of Glt_{Ph} is approximately 36% identical to the human glutamate transporters with many of the residues that have been previously identified as crucial for the transporter function and also chloride permeation being conserved. Thus, Glt_{Ph} provides a good working model for predicting the structure of the human glutamate transporters and how they work. The Glt_{Ph} protein forms a homotrimeric complex in the shape of a bowl sitting within the

† This work was supported by the Australian National Health and Medical Research Council Project Grant 307604 and Fellowship 358711 to R.J.V.

* Address correspondence to this author. E-mail: robv@med.usyd.edu.au. Phone: +61-2-93516734. Fax: +61-2-93513868.

[1] Abbreviations: EAAT1, excitatory amino acid transporter 1; TM, transmembrane domain; TBOA, DL-*threo*-*β*-benzyloxyaspartate; OTV, oocyte transcription vector; NMDG, *N*-methyl-D-glucamine.

10.1021/bi700647f CCC: $37.00
Published on Web 08/04/2007

membrane with an aqueous basin facing the extracellular solution and a pointed wedge structure facing the intracellular solution. The protomers contain a number of unusual secondary structure features. TM1−6 form a distorted cylindrical structure, with TM7−8 and two hairpin-loop structures, HP1 and HP2, sitting within the cylinder and being responsible for glutamate transport (*10*, *11*). In a recent study it was demonstrated that Glt_{Ph} also allows an uncoupled chloride conductance (*12*). Furthermore, a S65V mutation within TM2 of Glt_{Ph} (corresponds to S103 in TM2 of EAAT1) impaired the chloride conductance, which suggests that the structural basis for chloride permeation may be conserved between the bacterial and mammalian transporters (*12*). The residues within TM2 that have been postulated to form the chloride permeation pathway are in the outer shell of the protomer and face into the aqueous accessible lumen (*9*, *10*) and may come in contact with HP1 and the intracellular edge of TM7.

In this study, the substrate-bound form of the Glt_{Ph} crystal structure (*10*) was used as a structural template to create an EAAT1 homology model which was then used to identify a number of charged residues that may be in close proximity to the polar residues that influence anion permeation of EAAT1 and may also affect channel function. Neutralization, or reversing the charge, of D272 in TM5 and K384 and R385 in TM7 had no effect on substrate binding and translocation but increased the amplitude of the substrate-activated anion current and also the substrate-independent "leak" current. These results identify additional domains that are involved in anion channel function and also provide hints as to how substrate binding leads to channel activation.

MATERIALS AND METHODS

Chemicals. DL-*threo*-β-Benzyloxyaspartate (TBOA) was obtained from Tocris (Bristol, U.K.). Restriction enzymes were purchased from Progen Industries Ltd. (Queensland, Australia). D-[2,3-^{3}H]Aspartic acid (specific activity = 1.41 Ci/mmol) was obtained from Amersham Biosciences (Piscataway, NJ). All other chemicals were obtained from Sigma Chemical Co. (Sydney, Australia) unless otherwise stated.

Oocyte Preparation. Xenopus laevis frogs were obtained from Xenopus Express (Haute-Loire, France). The frogs were anesthetized with 0.17% 3-aminobenzoic acid ethyl ester for approximately 10−20 min. Ovarian sacs were removed and rinsed several times in OR-2 (82.5 mM NaCl, 2 mM KCl, 1 mM $MgCl_2 \cdot 6H_2O$, 5 mM HEPES hemisodium salts, pH 7.55). Oocytes were isolated following denuding of overlaying follicle cells by agitation for 2−3 h in collagenase A (2 mg/mL) (Boehringer, Mannheim) in OR-2. Oocytes were rinsed several times in OR-2 solution followed by several rinses in ND96 wash solution (96 mM NaCl, 2 mM KCl, 1 mM $MgCl_2$, 1.8 mM $CaCl_2$, 5 mM HEPES hemisodium salts, 2.5 mM sodium pyruvate, 0.5 mM theophylline). Oocytes were stored in ND96 supplemented with 50 μg/mL gentamycin in 35 mM culture dishes at 16−18 °C with shaking. This procedure followed a protocol approved under the Australian Code of Practice for the Care and Use of Animals for Scientific Purposes.

Molecular Biology. EAAT1 was cloned into the plasmid oocyte transcription vector pOTV (*13*), and site-directed mutagenesis was performed using the QuikChange site-directed mutagenesis kit (Stratagene, Cedar Creek, TX). Primers were designed and synthesized by Sigma Genosys (Sydney, Australia), and all mutations were sequenced on both strands by dye terminator cycle sequencing at the University of Sydney Prince Alfred Macromolecular Analysis Centre (SUPAMAC) in an ABI PRISM 3700 analyzer. DNA was prepared using Qiagen mini prep kit (Qiagen Pty Ltd., City, Australia). The wild-type and mutant transporter cDNA were linearized with *Spe*I and cRNA transcribed with T7 RNA polymerase using the mMessage mMachine kit (Ambio Inc., Austin, TX).

Electrophysiology. Fifty nanoliters (10−50 ng) of wild-type or mutant cRNA was injected using a microinjector (Drummond Nanaject; Drummond Scientific Co., Broomall, PA) into defoliculated stage V−VI oocytes harvested from *X. laevis*. Currents were recorded 2 days later using the two-electrode voltage clamp method with a Geneclamp 500 amplifier (Axon instruments, Foster City, CA). Data were recorded using Chart (ADI Instruments) and Clampex (Axon Instruments) software and analyzed using the Clampfit software program (Axon Instruments).

D-*[^{3}H]Aspartate Uptake Assays.* Uptake of D-[^{3}H]aspartate was measured in oocytes expressing wild-type and mutant transporters and uninjected cells. D-[^{3}H]Aspartate (100 μM) was applied to each oocyte for 60 s while under voltage clamp conditions at −100 mV. Oocytes were then washed with ND96 for at least 3 min before being removed from the bath and lysed with 50 mM NaOH, and then 4 mL of scintillation fluid was added. Radioactive counts were measured using a TRI-CARB1500 scintillation counter.

Substrate-Activated Conductances. The current−voltage relationships for substrate-elicited conductance were determined by subtraction of steady-state current measurements in the absence of substrate (i.e., from −30 mV to potentials between −100 and +60 mV in 10 mV intervals) from corresponding current measurements in the presence of substrate.

Na^+-Dependent D-*Aspartate-Activated Conductances*. Na^+-dependent D-aspartate activated whole cell currents were recorded in oocytes expressing wild-type and mutant EAAT1 transporters. Current−voltage relationships were measured in the presence 100 μM D-aspartate in 0, 10, 36, 60, and 96 mM $NaNO_3$ with 96, 86, 60, 36, and 0 mM $NMDGNO_3$ solutions, respectively.

Anion Permeability Experiments. Current−voltage relationships were measured in the presence 100 μM D-aspartate in 10 mM NaCl, NaBr, NaI, or $NaNO_3$ with 86 mM sodium D-gluconate, 2 mM KCl, 1.8 mM $CaCl_2 \cdot 2H_2O$, and 5 mM HEPES, pH 7.5, and also in the same buffers in the absence of D-aspartate as described above. The recordings were made with the bath grounded with a 1 M KCl agar bridge connected to a 1 M KCl reservoir to minimize offset potentials. The permeability ratios for Br^-, I^-, and NO_3^- relative to chloride were calculated as previously described (*9*). This is calculated by first subtracting the substrate current (*e*-fold per 41 ± 2 mV for wild-type EAAT1; see Table 1 for similar values for the mutant transporters) from the substrate-activated net current to obtain the anion current. Using the reversal potential of various anion currents and assuming that the intracellular Cl^- concentration is 41 mM (*14*, *15*), the permeability ratio of various anions (i.e., Br^-,

Table 1: Kinetic and Electrophysiological Properties of Wild-Type and Mutant EAAT1 Transporters

	$K_{0.5}$(L-glutamate) (μM)	[^{3}H]aspartate uptake (pmol oocyte^{-1} min^{-1})	voltage dependence of transport component (*e*-fold per *x* mV)	E_{rev} (mV)	
				Cl^-	NO_3^-
EAAT1	22.0 ± 3.2	135 ± 23	41 ± 2[d]	8.3 ± 1.7	−70.0 ± 0.0
R268A	20.0 ± 3.8	88 ± 51	nd[e]	6.3 ± 1.1	−65.8 ± 1.2
D272A	18.9 ± 1.3	51 ± 1	43 ± 8	−11.3 ± 1.1[b]	−65.5 ± 1.3
D272K	27.9 ± 2.0	107 ± 9	44 ± 3	−5.0 ± 3.5[a]	−62.5 ± 4.8
K384A	33.1 ± 3.8	283 ± 19	53 ± 3[c]	20.0 ± 3.5[b]	−53.8 ± 2.4[b]
K384D	2.6 ± 0.1	79 ± 9	42 ± 3	30.0 ± 0.0[b]	−58.8 ± 1.3[a]
R385A	15.7 ± 2.1	69 ± 10	48 ± 1[a]	−2.5 ± 1.3	−70.0 ± 0.0
R385D	6.8 ± 1.1	75 ± 5	61 ± 8[c]	21.3 ± 4.3[a]	−61.3 ± 1.3
S103V[d]	13.0 ± 2.3	24 ± 2	nd	61.3 ± 5.0[c,d]	−39.0 ± 3.0[c,d]

[a] $P < 0.05$ when compared with wild-type EAAT1. [b] $P < 0.01$. [c] $P < 0.001$. [d] Data obtained from ref *9*. [e] nd, not determined.

I^-, NO_3^-) and Cl^- can be calculated using the Goldman−Hodgkin−Katz equation (*16*):

$$E_{rev} = (RT/-ZF) \ln[(P_{X^-}[X^-]_{out})/(P_{Cl^-}[Cl^-]_{in})]$$

where E_{rev} is the reversal potential of the substrate-activated current in the presence of extracellular anion X^-, P_{X^-} is the permeability of anion X^-, P_{Cl^-} is the permeability of Cl^-, $[A^-]_{out}$ is the concentration of anion A outside the cell, $[Cl^-]_{in}$ = 41 mM (*5*), *R* is the noble gas constant, *T* is temperature in kelvin, *F* is Faraday's constant, and $-Z$ is the number of charges on the anion.

TBOA-Blockable Leak Conductance. TBOA (50 μM) was applied to oocytes expressing wild-type or mutant transporter, and their current−voltage relationship was measured by subtracting the TBOA-blockable current from the steady-state current in the absence of TBOA as described above.

Data Analysis. Current responses were fitted by least squares as a function of substrate concentration to (*I*) to

$$I/I_{max} = [S]/(K_{0.5} + [S])$$

where I_{max} is the maximal current generated at a specific membrane potential, $K_{0.5}$ is the concentration of substrate that generates half-maximal current, and [S] is the substrate concentration. All values presented are means of at least four cells ± SEM. Analysis of all kinetic data was carried out using Kaleidagraph Software version 3.09 and Microsoft Office Excel 2003. One-way analysis of variance (ANOVA) with a Dunnett's post hoc test was performed using Prism GraphPad (GraphPade Software Inc.) to assess difference in the means. *P* values less than 0.05 were taken to be significant: *, $P < 0.05$, **, $P < 0.01$, ***, $P < 0.001$.

Molecular Modeling. A model of the structure of EAAT1 was generated by DeepView (*17*) based on a manual sequence alignment of EAAT1 and Glt_{Ph} (*10*). The homology structure was refined by SWISS-MODEL (*17*).

RESULTS

Generation of an EAAT1 Homology Model. The amino acid sequence of EAAT1 has approximately 36% of residues that are conserved with the sequence of the bacterial aspartate transporter Glt_{Ph} (*10*), with the degree of conservation considerably higher in functionally important domains. An EAAT1 structural model was generated using the program DeepView by using the structure of the substrate-bound form of Glt_{Ph} as a template. In the EAAT1 amino acid sequence, there are approximately 100 amino acid residues between TM 4b and 4c that are not found in bacterial aspartate transporters. This region was deleted to allow the EAAT1 sequence to be threaded onto the Glt_{Ph} structure. The homology structural model of the EAAT1 protomer generated is presented in Figure 1A. All of the residues that have previously been identified as playing a role in either transport or channel functions of EAAT1 are located in positions that correspond to the equivalent residues in Glt_{Ph}. S103 and T106 in TM2 have previously been identified as residues that influence ion permeation of the anion channel of EAAT1. The minimal pore diameter of the anion channel has been estimated to be 5.8 Å (*14*), and so we identified side chains in the homology model that were approximately 5 Å from S103 and T106. Three charged residues were predicted to be close to S103 and T106: R268 and D272 in TM5 and K384 in TM7 (the side chains of R268 and D272 are 3.3 and 4.3 Å from the hydroxyl group of T106, respectively, and the side chain of K384 is 6.9 Å from the hydroxyl of S103) (Figure 1). D112 in the intracellular loop between TM2 and TM3 of EAAT1 has previously been postulated to be involved in gating of the anion channel, and from the EAAT1 homology structure, the closest polar or charged residue to D112 that is not in TM2 is R385 in TM7 (the distance between the carboxyl group of D112 and the guanidino group of R385 is 7.1 Å). We investigated the role of these charged residues in anion channel function by mutating each of the

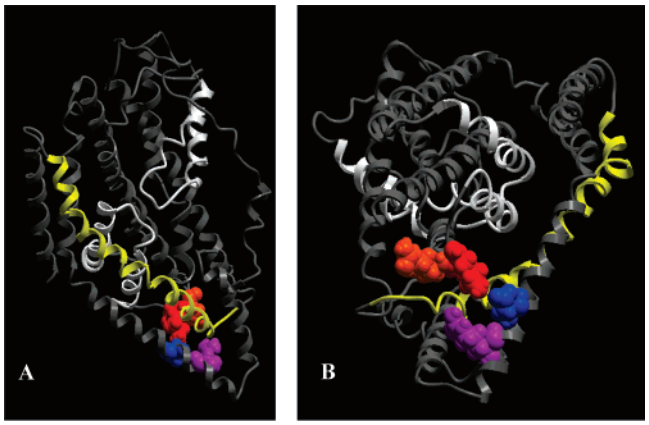

FIGURE 1: Structure of a homology model of an EAAT1 protomer. Hairpin loops 1 and 2 are highlighted in white; transmembrane 2 is highlighted in yellow. The following residues were identified to be in close proximity to S103, T106 in TM2, and D112 in the TM2−TM3 loop (residues not shown): R268 (purple), D272 (blue), K384 (red), and R385 (orange). (A) Side view of transporter protomer. (B) View of the protomer from the internal surface showing the predicted positions of R268, D272, K384, and R385.

residues to an uncharged residue (i.e., alanine) or a reverse charged residue (either aspartate or lysine) and studied the transport and channel properties of the mutant transporters expressed in *X. laevis* oocytes.

Neutralizing or Reversing the Charges of D272, K384, and R385 Alters the Anion Channel of EAAT1. Application of glutamate to the R268, D272, and R385 mutants generated inward currents at −60 mV of similar amplitude to wild-type transporters. The $K_{0.5}$ for glutamate-activated currents for these mutants, the rates of [^{3}H]aspartate transport, and the voltage dependence of transport currents (see below) are all similar to the wild-type EAAT1 values (see Table 1). For the K384A mutant, larger transport currents and faster rates of D-[^{3}H]aspartate transport were observed, suggesting that higher levels of expression were achieved with this mutant. However, the $K_{0.5}$ for the K384A mutant was similar to that of the wild type. The K384D mutant has an 8-fold reduction in EC_{50} for glutamate compared to wild type but still retains significant transport activity. These results suggest that these residues are unlikely to be directly involved in substrate translocation. In the following experiments we have used D-aspartate as the substrate because D-aspartate generates a significantly greater anion conductance than L-glutamate in EAAT1, which allows more reliable measures of anion channel activity (*9*, *14*). Application of substrate to oocytes expressing EAAT1 generates a current that is the sum of the substrate-transport current and the substrate-activated anion current. It is possible to increase the amplitude of the substrate-activated anion conductance by using NO_3^- instead Cl^- as the external anion because NO_3^- ions are more permeant through the transporter than Cl^- (*5*). The amplitudes of the D-aspartate-activated outward currents at +60 mV in the presence of NO_3^- for the mutants D272A, D272K, and R385A are greater than those for wild-type EAAT1 [Figure 2; the relative increases in current amplitude were (2.7 ± 0.2)-, (3.9 ± 0.3)-, and (2.3 ± 0.1)-fold greater than wild type, respectively], which suggests that the anion currents of these three mutants are altered compared to wild-type transporters.

To gain more insight into the nature of the alterations in channel function of the mutant transporters, it is necessary to isolate the two components of the substrate-activated currents. The current due to D-aspartate was estimated using the method described by Ryan et al. (*9*). First, 100 μM D-[^{3}H]-aspartate was applied to oocytes voltage clamped at −100 mV and expressing the transporters. The amount of D-[^{3}H]-aspartate uptake and the total charge transfer associated with D-[^{3}H]aspartate application were measured. D-Aspartate transport is coupled to the cotransport of 3 Na^+ and 1 H^+ and the countertransport of 1 K^+, which generates a net transfer of 2 charges per D-aspartate transport. The proportion of total current at −100 mV that is due to coupled D-aspartate transport was then estimated from the charge to flux ratio (Figure 3). The voltage dependence of D-aspartate transport by EAAT1 and the mutant transporters was estimated by varying the extracellular chloride concentration and measuring the current at the calculated chloride reversal potential for each chloride concentration, assuming that the internal chloride concentration is 41 mM (*14*). The current at each of these potentials will have no contribution from chloride ions and will be due solely to the coupled transport current. The transport currents were then fit to an exponential

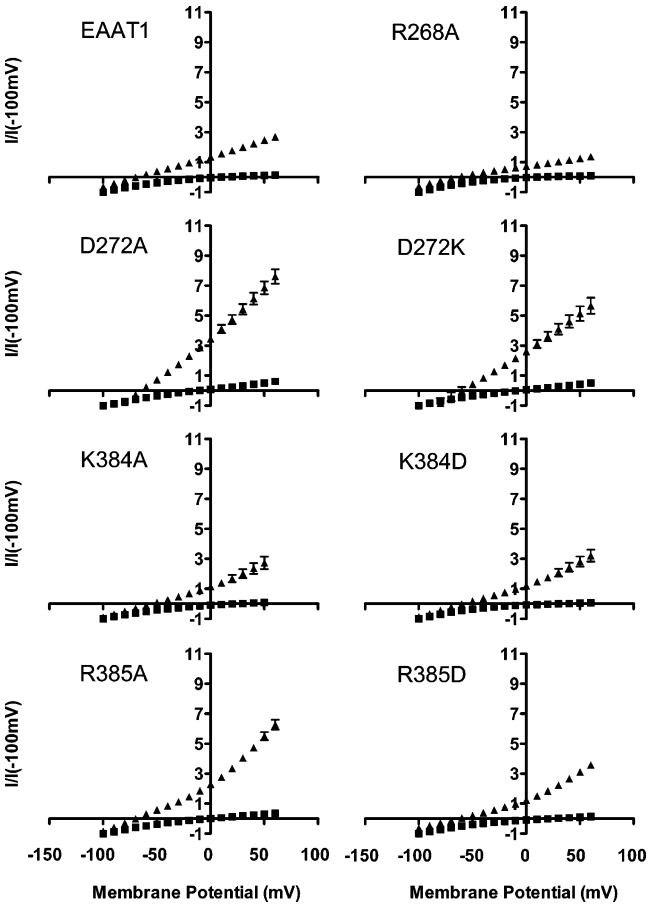

FIGURE 2: Current−voltage relationships elicited by 100 μM D-aspartate in Cl^- and NO_3^- solutions. Recordings were made in 96 mM Cl^- (closed squares) or 96 mM NO_3^- (closed triangles). Currents (*I*) are normalized to the current generated by 100 μM D-aspartate at −100 mV in 96 mM Cl^-.

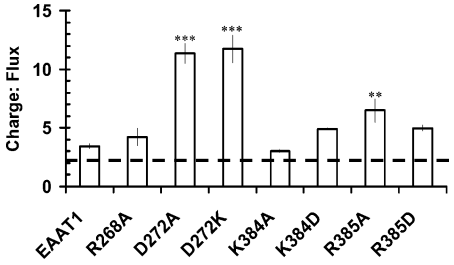

FIGURE 3: Charge to flux ratio of wild-type and mutant transporters. 100 μM D-[^{3}H]aspartate was applied for 1 min to oocytes voltage clamped at −100 mV and expressing wild-type and mutant glutamate transporters. The number of charges translocated (charge) per D-aspartate molecule (flux) was calculated. A charge/flux ratio of 2 is due to substrate transport (i.e., a net two positive charges are transported per transport cycle; this is represented by the dashed line). The remainder of the charge/flux is due to the uncoupled anion flux (**, $P < 0.01$; ***, $P < 0.001$; when compared with wild-type EAAT1; $n \geq 4$). 96 mM Cl^- solution was used in this experiment.

function. For wild-type EAAT1 there is an *e*-fold change per 41 mV(*9*, *14*), which was used to calculate the current due to transport at each membrane potential. Similar *e*-fold changes were obtained for each of the mutant transporters (see Table 1). The calculated transport currents were then subtracted from the total current at each membrane potential to obtain the D-aspartate-activated anion current (Figure 4).

The D272A, D272K, and K384D mutants showed the most marked increases in amplitude of the anion conductances

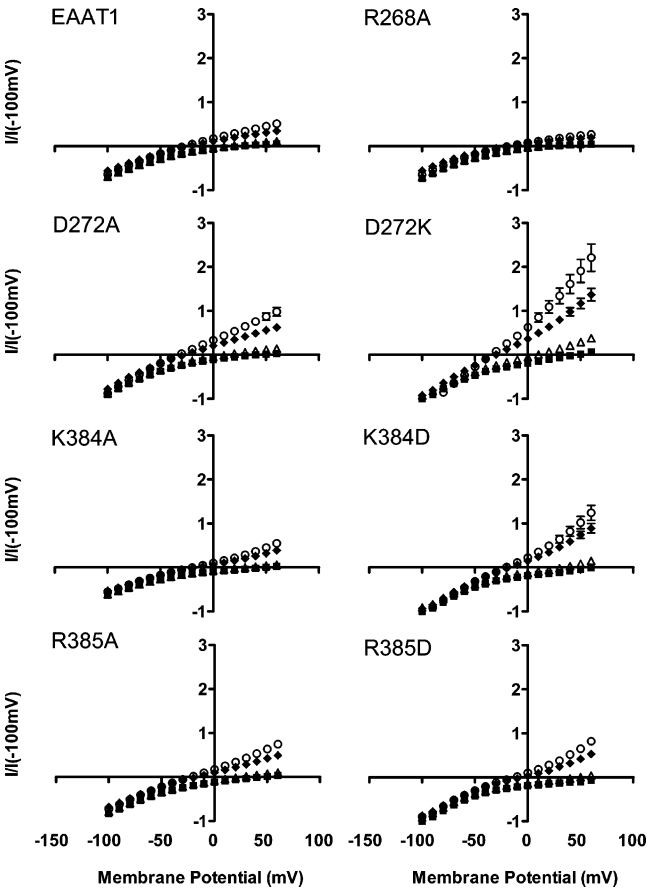

FIGURE 4: Anion currents generated by 100 μM D-aspartate for each of the mutant transporters. Currents were measured in the presence of 10 mM external anions Cl^- (closed squares), Br^- (open triangles), I^- (closed diamonds), and NO_3^- (open circles), and the anion component of the D-aspartate-elicited current was isolated as described in the text.

compared to wild type (Figure 4). These increases in amplitude of the anion currents of the mutant transporters could be due to either altered anion permeability of the mutants compared to wild-type EAAT1 or altered gating of the channel to allow more anions to pass. The anion permeabilities for NO_3^-, I^-, and Br^- relative to Cl^- were calculated from the reversal potential of the D-aspartate-activated anion conductances measured in the presence of 10 mM Cl^-, Br^-, I^-, and NO_3^- for each of the eight mutant transporters (Figure 4, Table 2). In some cases statistical differences were observed, but when compared to the results of the S103V mutant (*9*), the magnitude of these changes was not as great. With the exception of R385D mutant, no changes in the rank order of permeabilities were observed in the mutants. Therefore, these results suggest that these residues are unlikely to play a major role in the interactions between each of the anions and the pore of the transporter. The increased amplitude of the anion currents for the mutant transporter could be due to faster rates of anion permeation or altered gating of the channel, but at present we are unable to distinguish between these two possibilities.

In addition to the substrate-activated anion conductance of EAAT1, anions leak through the transporter in the absence of substrate. This leak conductance is most readily observed by blocking the current with the glutamate transport blocker TBOA (*9*, *18*) (Figure 5). The relative anion permeabilities of the leak conductance are significantly different from the substrate-activated anion conductance (*9*, *19*), which suggests that the lining of the pore of the channel changes depending on whether or not substrate is bound to the transporter. We investigated the anion leak currents of the mutant transporters and compared them to wild-type transporters. In the presence of 96 mM NO_3^- the amplitude of the leak current was significantly greater for the K384A and R385A mutant transporters compared to wild-type EAAT1 [Figure 5; the relative current amplitudes at +60 mV were (6.9 $\pm$ 0.9)- and (9.9 $\pm$ 0.9-fold greater than wild-type EAAT1]. We also investigated whether reversing the charge on these residues would cause further increases in the amplitudes of the leak currents. However, while the K384D and R385D mutants did show increased amplitudes of the leak conductances compared to wild-type EAAT1 [(2.0 $\pm$ 0.4)- and (1.8 $\pm$ 0.2)-fold increases], they were smaller than the respective alanine mutants. In the case of the D272 mutants, the amplitudes of the leak currents were significantly greater than wild type [(15.9 $\pm$ 2.3)- and (10.4 $\pm$ 0.8)-fold increases compared to EAAT1, respectively].

We measured the relative anion permeabilities for the leak currents for each of the mutants using 10 mM Cl^-, Br^-, I^-, or NO_3^- in the external solution as described above, and the results are presented in Table 2. Although the amplitudes of the leak currents were significantly greater for the D272, K384, and R385 mutant transporters compared to wild type, the relative anion permeabilities were not significantly different. Thus, it appears that the mutations do not affect anion permeability. At present we are unable to determine whether the increased amplitudes are due to greater anion permeation rates or altered gating of the anion channel. It is interesting to note that the K384A mutant does not affect the amplitude of the D-aspartate-activated anion current but does affect the amplitude of the leak current.

Another explanation for the altered amplitudes of the leak and substrate-activated anion currents is that the mutations may alter the affinity of Na^+ for the transporter and thereby alter the Na^+ dependence for activation of the currents. We investigated this possibility by measuring the Na^+ dependence for activation of the substrate-gated anion current. Na^+ ions were replaced with $NMDG^+$, and NO_3^- was used as the anion to enhance the amplitude of the anion current. Currents were measured at +60 mV, a membrane potential at which the amplitude of the current is predominantly due to the substrate-activated anion current with minimal contributions from the transport current. Under these conditions, the $K_{0.5}$ values for Na^+-dependent activation of the anion currents were similar for all of the mutants and were not significantly different to the wild-type transporter (Table 3). These results suggest that the differences in amplitude of the substrate-activated anion conductance in the mutants are unlikely to be due to altered Na^+ affinity. While the $K_{0.5}$ values are not significantly different, changes in the Hill coefficient for Na^+ were observed for the K384A and R385A mutants compared to wild type (Table 3). The leak current associated with EAAT1 can be measured using two methods. The first method is to increase the Na^+ concentration and measure the increase in current amplitude; however, this method is complicated by the presence of an endogenous anion current in oocytes which contributes a large proportion of the current and makes isolation of the transporter leak

Table 2: Relative Anion Permeability Ratios for D-Aspartate-Activated Conductances and TBOA-Blocked Conductances of Wild-Type and Mutant EAAT1 Transporters

	D-aspartate				TBOA			
	$P_{Br/Cl}$	$P_{I/Cl}$	$P_{NO_3/Cl}$	n	$P_{Br/Cl}$	$P_{I/Cl}$	$P_{NO_3/Cl}$	n
EAAT1	2.5 ± 0.1	10.7 ± 0.5	12.5 ± 0.6	6	1.0 ± 0.0	1.4 ± 0.1	1.6 ± 0.1	5
R268A	2.5 ± 0.2	8.4 ± 0.6	8.4 ± 0.6^b	5	0.6 ± 0.1^a	1.0 ± 0.3	1.1 ± 0.1	5
D272A	2.5 ± 0.2	11.5 ± 0.8	15.2 ± 0.6	4	1.1 ± 0.1	1.8 ± 0.2	1.8 ± 0.2	5
D272K	3.2 ± 0.2^a	14.3 ± 0.6^c	16.6 ± 0.9^b	6	1.0 ± 0.1	1.6 ± 0.1	1.8 ± 0.1	5
K384A	2.3 ± 0.1	13.8 ± 0.4^b	16.6 ± 0.5^b	6	0.9 ± 0.1	1.2 ± 0.0	1.2 ± 0.0	4
K384D	1.6 ± 0.1^c	10.3 ± 0.9	10.3 ± 0.9	5	1.0 ± 0.0	1.4 ± 0.1	2.0 ± 0.5	4
R385A	1.7 ± 0.1^c	8.9 ± 0.4	$11.3 + 0.4$	6	1.0 ± 0.0	1.3 ± 0.0	1.4 ± 0.1	4
R385D	0.9 ± 0.1^c	11.2 ± 0.3	14.6 ± 0.0^b	4	1.1 ± 0.1	1.4 ± 0.1	1.5 ± 0.1	6
S103V[d]	1.1 ± 0.2^b	2.7 ± 0.8^c	3.1 ± 0.2^c	5				

[a] $P < 0.05$ when compared with wild-type EAAT1. [b] $P < 0.01$. [c] $P < 0.001$. [d] Data obtained from ref *9*.

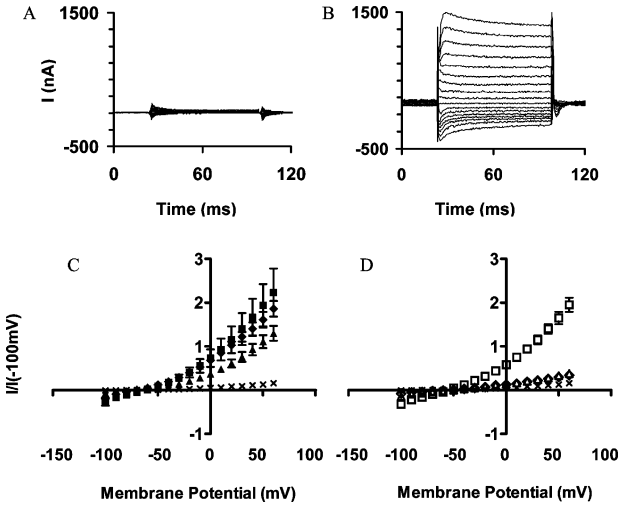

FIGURE 5: The TBOA blocked leak currents. Representative current traces of the TBOA-blocked leak currents in 96 mM NO_3^- buffer of EAAT1 (A) and D272A (B). TBOA blocked currents in 96 mM NO_3^- standardized using 100 μM D-aspartate activated currents at -100 mV membrane potential for the wild type and alanine mutants (C) and wild type and reverse charge mutants (D). Key: (C) wild-type EAAT1 (crosses), D272A (closed squares), K384A (closed triangles), and R385A (closed diamonds); (D) wild-type EAAT1 (crosses), D272K (open squares), K384D (open triangles), and R385D (open diamonds).

Table 3: $K_{0.5}$ and Hill Coefficients for Na^+ [a]

	$K_{0.5}$ (μM)	Hill coefficient
EAAT1	66.3 ± 1.9	2.1 ± 0.1
D272A	89.3 ± 18.9	1.7 ± 0.1
K384A	71.4 ± 15.6	1.2 ± 0.2^c
R385A	69.7 ± 4.7	1.5 ± 0.0^b

[a] Currents measured at +60 mV using 100 μM D-aspartate with variable [Na^+]. [b] $P < 0.05$ when compared with wild-type EAAT1. [c] $P < 0.01$.

current problematic. The second method utilizes TBOA to block the transporter leak current and thereby isolate the current mediated by the transporter. However, TBOA binding to EAATs is Na^+ dependent (*20*), and so the ability to measure the Na^+ dependence of the leak is compromised. Thus, we are unable to determine whether the Na^+-dependent activation of the leak current is altered in the mutant transporters compared to the wild-type transporter.

DISCUSSION

In this study we have used a homology model of the human glutamate transporter EAAT1 to identify amino acid residues that may be involved in formation and gating of the intrinsic anion channel. Mutations of three residues, D272, K384, and R385, were found to increase the amplitudes of both the substrate-activated anion current and the leak current without causing significant changes in the relative anion permeability of the channels or the rates of glutamate transport. These results suggest that the mutations have either altered the gating mechanism of the channel or increased the rate of anion permeation through the transporter.

The recently determined crystal structures of the bacterial aspartate transporter Glt_{Ph} provide the basis for beginning to understand the molecular basis for transporter functions. The published structure of Glt_{Ph} represents two conformations of the transporter: one with substrate and two Na^+ ions bound and the other with the transport blocker TBOA and 1 Na^+ ion bound. This has provided information about how substrates and blockers bind to Glt_{Ph}, but a number of additional conformational states must also exist for the transporter to accomplish its function of transporting glutamate and various co- and countertransported ions across the membrane (*11*). Although we know that the conformation required for channel activation differs from that required for transport (*6*−*8*), it is not clear whether the crystal structure of the substrate-bound form of GltPh represents a conformational state involved in transport in channel activation. In the region that we focused on in this study, there are no major structural differences between the substrate- and blocker-bound conformations, and therefore we are unable to determine whether the structures depict an open or closed state of the channel. Therefore, while the EAAT1 homology model can provide hints as to regions that may be involved in transporter function, the model should be treated as a tool for making predictions that can be tested, if possible, by experimental means.

We used the model to predict residues that may be involved in the channel function of EAAT1. As both EAAT1 and Glt_{Ph} allow substrate-dependent anion fluxes through their respective transporters, presumably residues in similar regions of the two transporters fulfill this role. S103 of EAAT1 is conserved between the mammalian and bacterial transporters, and mutations of this residue in EAAT1 and the corresponding S65 of Glt_{Ph} impair chloride channel function (*12*). Of the residues identified in the current study as impacting on channel function, D272 is not conserved and is a N residue in Glt_{Ph} and also all other EAATs. We generated a D272N mutant in EAAT1, but there were no

changes in transport or channel function compared to wild-type EAAT1 (results not shown), which suggests that a D or a N at this position is sufficient, but an A or K residue alters channel function. The residues corresponding to K384 and R385 are conserved between the other EAATs, but in Glt_{Ph} the corresponding residues are I and G, respectively. It is difficult to rationalize how such different side chains could play similar roles, and therefore either this region is unlikely to be involved in channel function in Glt_{Ph} or the structures of this region of the two transporters may be quite different and other residues in Glt_{Ph} may serve the role of K384 and R385.

In a previous study we suggested that the D112A mutation in EAAT1 locked the anion channel in an open state such that a large constitutive leak current was observed and that application of substrate did not activate the channel further (*9*). In this study we have identified additional residues that in some ways appear to cause similar effects, but in other respects the effects are quite different. The D272A, D272K, K384A, and R385A mutants have large anion leak conductances that are similar to that observed for D112A. However, in contrast to the D112A mutant, the D272A and D272K mutants have significantly larger substrate-activated anion conductances compared to the wild type and also the D112A mutant. Thus, the D272A and D272K mutations may either facilitate opening of the anion channel or increase the rate of anion permeation both in the presence and also in the absence of substrate. To resolve which of these possibilities is most likely, it would be necessary to conduct noise analysis of the currents. Using this method, Wadiche and Kavanaugh (*14*) estimated that the single channel conductance is less than 1 fS. However, we have been unable to reliably measure such currents, and therefore, the answer to this question remains unresolved.

The alanine mutations of the three residues show some subtle differences, which may provide some hints as to the roles of TM5 and TM7 in gating of the anion channel. The D272A mutant showed the most marked changes in amplitudes of both the substrate-activated anion current and the anion leak current but showed no change in the EC_{50} for glutamate, the EC_{50} for Na^+, or the Hill coefficient for Na^+ dependence of the D-aspartate-activated anion current. While the K384A and R385A mutants did show changes in amplitudes of the anion current, they were not as marked as the D272A mutant, and in addition, the Hill coefficient for Na^+ dependence of the D-aspartate-activated anion current was reduced from 2.1 ± 0.1 to 1.2 ± 0.2 and 1.5 ± 0.0, respectively. While it is difficult to reliably interpret the significance of a change in Hill coefficient, this difference does suggest slightly altered interactions between Na^+ and the transporter compared to the wild-type transporter. D272 is in TM5 which is part of the outer shell region of the glutamate transporter, which is a region that has not previously been directly implicated in any functional role of the transporter (*10*). On the other hand, K384 and R385 are likely to be located at the intracellular edge of TM7, and residues in the extracellular half of TM7 have been implicated in substrate discrimination and cation binding (*10*, *21*, *22*), and therefore it is reasonable to suggest that parts of TM7 may undergo conformational changes during the transport process. If these changes are transmitted down to the intracellular end of TM7, then the K384A and R385A mutations may cause subtle changes in the way Na^+ is coupled to the substrate translocation and also channel activation.

The identification of amino acid residues from three different transmembrane domains of glutamate transporters that play a role in anion channel function provides some hints about how the channel structure may be formed and activity regulated. Yernool et al. (*10*) suggested that TM7, TM8, HP1, and HP2 are involved in ion-coupled glutamate transport and that these structural domains sit within an external distorted cylindrical structure made up of TM1−6. This study, our previous study (*9*), and the study of Ryan and Mindell (*12*) have identified residues from both the outer cylindrical structure (S103 in TM2 of EAAT1, S65 of TM2 in Glt_{Ph}, D112 in the TM2−TM3 intracellular loop, and D272 in TM5) and the inner translocation domain (R385 and K384 at the intracellular edge of TM7) that are involved in channel function. This interpretation is consistent with our previous study that demonstrated that a number of residues in TM2 form an aqueous accessible structure (*9*). Therefore, the channel may be formed by an aqueous cavity between the outer cylinder (TM2 and TM5) and the inner translocation domain (TM7, TM8, HP1, and HP2; see Figure 1B). Gating of the channel could then be brought about by movements of the inner translocation domain associated with the transport process being translated down through TM7 to K384 and R385 such that the conformations of D112 and D272 are altered to allow anion passage.

ACKNOWLEDGMENT

We are grateful for Kim Shaddick, Xin Liu, Kong Li, Hue Tran, and Suzanne Habjan for assistance in maintaining the *X. laevis* colony.

SUPPORTING INFORMATION AVAILABLE

One figure showing amino acid sequence alignments of EAAT1-3, ASCT1, and Glt_{Ph}. This material is available free of charge via the Internet at http://pubs.acs.org.

REFERENCES

1. Danbolt, N. (2001) Glutamate uptake, *Prog. Neurobiol. 65*, 1−105.
2. Zerangue, N., and Kavanaugh, M. P. (1996) Flux coupling in a neuronal glutamate transporter, *Nature 383*, 634−637.
3. Veruki, M. L., Morkve, S. H., and Hartveit, E. (2006) Activation of a presynaptic glutamate transporter regulates synaptic transmission through electrical signaling, *Nat. Neurosci. 9*, 1388−1396.
4. Fairman, W. A., Vandenberg, R. J., Arriza, J. L., Kavanaugh, M. P., and Amara, S. G. (1995) An excitatory amino-acid transporter with properties of a ligand-gated chloride channel, *Nature 375*, 599−603.
5. Wadiche, J. I., Amara, S. G., and Kavanaugh, M. P. (1995) Ion fluxes associated with excitatory amino acid transport, *Neuron 15*, 721−728.
6. Seal, R. P., Shigeri, Y., Eliasof, S., Leighton, B. H., and Amara, S. G. (2001) Sulfhydryl modification of V449C in the glutamate transporter EAAT1 abolishes substrate transport but not the substrate-gated anion conductance, *Proc. Natl. Acad. Sci. U.S.A. 98*, 15324−15329.
7. Ryan, R. M., and Vandenberg, R. J. (2002) Distinct conformational states mediate the transport and anion channel properties of the glutamate transporter EAAT-1, *J. Biol. Chem. 277*, 13494−13500.
8. Borre, L., Kavanaugh, M. P., and Kanner, B. I. (2002) Dynamic equilibrium between coupled and uncoupled modes of a neuronal glutamate transporter, *J. Biol. Chem. 277*, 13501−13507.
9. Ryan, R., Vandenberg, R., and Mitrovic, A. (2004) The chloride permeation pathway of a glutamate transporter and its proximity

to the glutamate translocation pathway, *J. Biol. Chem. 279*, 20742−20751.
10. Yernool, D., Boudker, O., Jin, Y., and Gouaux, E. (2004) Structure of a glutamate transporter homologue from Pyrococcus horikoshii, *Nature 431*, 811−818.
11. Boudker, O., Ryan, R. M., Yernool, D., Shimamoto, K., and Gouaux, E. (2007) Coupling substrate and ion binding to extracellular gate of a sodium-dependent aspartate transporter, *Nature 445*, 387−393.
12. Ryan, R. M., and Mindell, J. A. (2007) The uncoupled chloride conductance of a bacterial glutamate transporter homolog, *Nat. Struct. Mol. Biol. 14*, 365−371.
13. Arriza, J. L., Fairman, W. A., Wadiche, J. I., Murdoch, G. H., Kavanaugh, M. P., and Amara, S. G. (1994) Functional comparisons of three glutamate transporter subtypes cloned from human motor cortex, *J. Neurosci. 14*, 5559−5569.
14. Wadiche, J. I., and Kavanaugh, M. P. (1998) Macroscopic and microscopic properties of a cloned glutamate transporter/chloride channel, *J. Neurosci. 18*, 7650−7661.
15. Wadiche, J., Amara, S., and Kavanaugh, M. (1995) Ion fluxes associated with excitatory amino acid transport, *Neuron 15*, 721−728.
16. Hill, B. (2001) *Ionic Channels of Excitable Membranes*, 3rd ed., Sinauer Associates, Sunderland, MA.
17. Guex, N., and Peitsch, M. C. (1997) SWISS-MODEL and the Swiss-PdbViewer: an environment for comparative protein modeling, *Electrophoresis 18*, 2714−2723.
18. Shimamoto, K., Lebrun, B., Yasuda-Kamatani, Y., Sakaitani, M., Shigeri, Y., Yumoto, N., and Nakajima, T. (1998) DL-*threo*-β-benzyloxyaspartate, a potent blocker of excitatory amino acid transporters, *Mol. Pharmacol. 53*, 195−201.
19. Melzer, N., Biela, A., and Fahlke, C. (2003) Glutamate modifies ion conduction and voltage-dependent gating of excitatory amino acid transporter-associated anion channels, *J. Biol. Chem. 278*, 50112−50119.
20. Shimamoto, K., Otsubo, Y., Shigeri, Y., Yasuda-Kamatani, Y., Satoh, M., Kaneko, S., and Nakagawa, T. (2006) Characterization of the tritium labeled analog of L-*threo*-β-benzyloxyaspartate (TBOA) binding to glutamate transporters, *Mol. Pharmacol*. (in press).
21. Tao, Z., Zhang, Z., and Grewer, C. (2006) Neutralization of the aspartic acid residue Asp-367, but not Asp-454, inhibits binding of Na^+ to the glutamate-free form and cycling of the glutamate transporter EAAC1, *J. Biol. Chem. 281*, 10263−10272.
22. Grewer, C., Watzke, N., Rauen, T., and Bicho, A. (2003) Is the glutamate residue Glu-373 the proton acceptor of the excitatory amino acid carrier 1?, *J. Biol. Chem. 278*, 2585−2592.

BI700647F